

Pressure-induced structural, electronic, and magnetic effects in  $\text{BiFeO}_3$ 

O. E. Gonzalez-Vazquez and Jorge Iniguez

Institut de Ciència de Materials de Barcelona (ICMAB-CSIC), Campus UAB, 08193 Bellaterra, Spain

We present a first-principles study of multiferroic  $\text{BiFeO}_3$  at high pressures. Our work reveals the main structural (change in Bi's coordination and loss of ferroelectricity), electronic (spin crossover and metallization), and magnetic (loss of order) effects favored by compression and how they are connected. Our results are consistent with the striking manifold transition observed experimentally by Gavriluk et al. [Phys. Rev. B 77, 155112 (2008)] and provide an explanation for it.

PACS numbers: 64.70.K-, 75.30.Wx, 75.80.+q, 71.15.Mb

Room-temperature multiferroic  $\text{BiFeO}_3$  (BFO) is one of the most intensively studied materials of the moment. BFO is among the most promising multiferroics from the applications perspective, and the latest results regarding its fundamental properties [1] and the engineering possibilities it offers [2] continue to fuel the interest in it.

Indeed, recent works suggest the correlations between the structural, electronic, and magnetic properties of  $\text{BiFeO}_3$  are not understood yet. We have evidence for a large sensitivity of BFO's conductivity to magnetic order [1, 3], a metal-insulator (MI) transition driven by structural changes at high temperatures [4], metallicity at ferroelectric domain walls [5], and even a spin-glass phase below 150 K [6]. Yet, the results most revealing of the complex interactions in BFO may be those of Gavriluk et al. [7, 8]. These authors observed a pressure-driven diuse transition, occurring at room temperature in the 40-50 GPa range, that involves a structural change, loss of magnetic order, and metallization. The driving force behind such transformations, tentatively attributed to a spin crossover of  $\text{Fe}^{3+}$ , remains to be clarified.

Here we report on a first-principles study of the high-pressure behavior of BFO in the limit of very low temperatures (nominally, 0 K). Our results reproduce the essential observations of Gavriluk et al., thus revealing the mechanisms that can lead to a manifold (structural/electronic/magnetic) transition in this material.

**Methods.** We used the local density approximation (LDA) [9] to density functional theory as implemented in the code VASP [10], including the so-called LDA+U correction of Dudarev et al. [11] for a better treatment of iron's 3d electrons. The technicalities of our calculations [12] are standard, but our use of the LDA+U asks for a comment: In this work we compared the energies of different electronic phases (insulating/metallic) in which the  $\text{Fe}^{3+}$  ions display different spin states. Doing this accurately constitutes a challenge for any ab initio approach; in particular, while commonly used to study such problems, the computationally-efficient LDA+U should be employed with caution in this context. For this reason, we repeated all our calculations for different values of the U parameter in the 0-4 eV range, and thus make sure our qualitative conclusions are reliable. (Unless oth-

erwise indicated, the reported results are for  $U = 3$  eV.)

Phase transitions in BFO under moderately high pressures have been studied theoretically [3]. In this work, however, we were not interested in the relatively mild effects so far investigated. Rather, we wanted to determine whether pressure may induce profound changes in the electronic structure of the compound. Thus, we restricted our simulations to the 10-atom cell of the R3c phase of BFO stable at ambient conditions (see inset in Fig. 1), assuming this is enough to capture the phenomena of interest. Then, as a function of volume (i.e., pressure), we performed structural relaxations for a variety of atomic, electronic, and magnetic configurations. That allowed us to identify a large number of possible phases and determine their relative stability and properties. As done in other first-principles studies [13, 14], we neglected the long-period spin cycloid in BFO.

**Structural and spin transitions.** Figure 1 displays our results for the equation of state of the BFO phases we found to be stable in some pressure range. The obtained pressure-driven transitions are better visualized in Fig. 2, which shows the pressure dependence of the key properties. At ambient and moderately high pressures we obtained the usual ferroelectric R3c phase of BFO, with G-type AFM order and  $\text{Fe}^{3+}$  in a high-spin (HS) state. Then, we found that at about 36 GPa BFO undergoes a

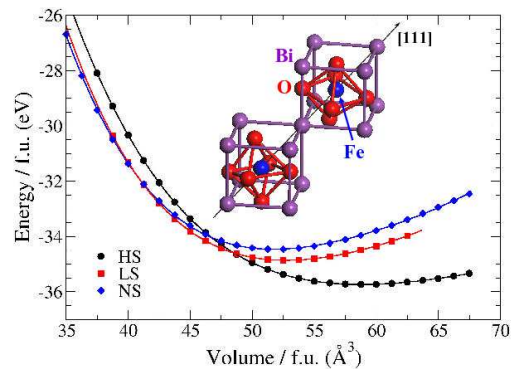


FIG. 1: (color online).  $E(V)$  curves for the BFO phases here considered (see text). Inset: structure of the ferroelectric R3c phase of BFO stable at ambient conditions.

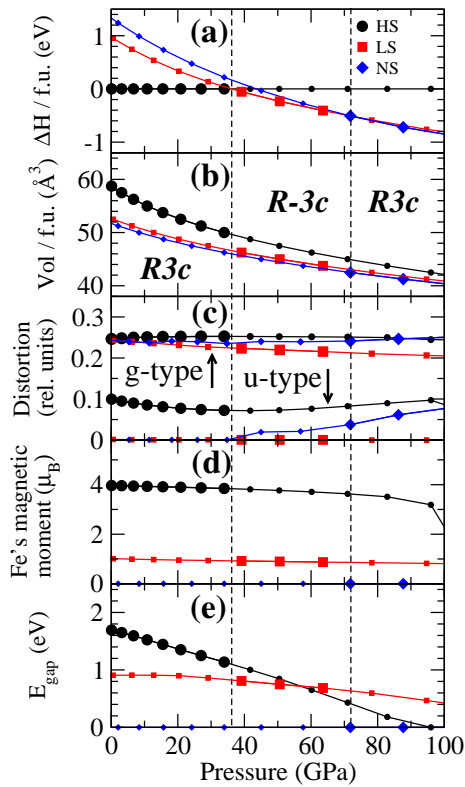


FIG. 2: (color online). Pressure-dependence of the enthalpy (a), volume (b), structural distortions with respect to the ideal cubic perovskite structure (c), Fe's localized magnetic moment (d), and electronic band gap (e) for the phases of BFO here considered (see text). Dashed vertical lines mark the transition pressures. Bigger symbols indicate which phase is stable. Panel (a): We take as the zero of enthalpy the pressure-dependent result for the HS phase. Panel (c): For all phases, the upper (resp. lower) symbols correspond to the g-type (resp. u-type) distortions (see text); distortions in units relative to the pressure-dependent lattice vectors. Panel (e): The highlighted area is suggestive of the subtleties pertaining to the value of  $E_{\text{gap}}$  in the LS phase (see text).

rst-order phase transition to a phase with the  $\text{Fe}^{3+}$  ions in a low-spin (LS) configuration. The concurrent drops in volume and iron's magnetic moment across the HS{LS transition can be seen, respectively, in Figs. 2b and 2d. (The magnetic moments are nearly pressure-independent within both the HS and LS phases.) Finally, a metallic phase with no localized magnetic moments, denoted as "NS phase" where NS stands for "No Spin", becomes stable above 72 GPa. Such a paramagnetic metallic phase is typical of transition-metal oxides at high pressures [15].

The main structural features of the obtained stable phases can be described in terms of g-type and u-type distortions of the ideal cubic perovskite structure, where g (resp. u) stands for gerade or even under inversion (resp. ungerade or odd under inversion). The evolution with pressure of the distortions thus quantified is shown in Fig. 2c. For all the phases, the g-type distor-

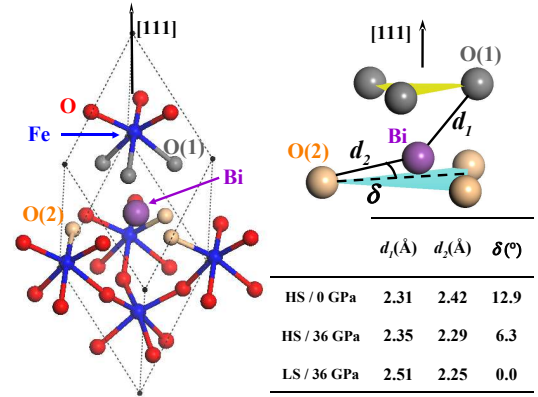


FIG. 3: (color online). Left: surroundings of Bi in the BFO structure. The six nearest-neighbor oxygens are split in two groups, denoted O(1) and O(2) and colored differently, each of which is composed of three symmetry-related atoms that form a plane perpendicular to the [111] direction. Right: Structural parameters relevant to the HS{LS transition.

tions are essentially oxygen-octahedron rotations as those occurring in the ferroelectric R3c phase of BFO at ambient pressure; our calculations show such rotations remain present under compression. The u-type displacements in the HS phase correspond to the usual ferroelectric distortion of BFO, dominated by the stereochemical activity of bismuth: the Bi atoms move along the [111] direction to approach the three O atoms forming a face of the neighboring oxygen octahedron. In the LS phase, though, we find a null u-type distortion (R3c space group), which reflects a change in bismuth's coordination. As shown in Fig. 3, the LS phase presents  $\text{BiO}_3$  planar groups in which the three oxygens binding with one Bi atom belong to three different  $\text{O}_6$  octahedra. Such planar groups are also present in the NS phase, but there they co-exist with a u-type displacement, along the rhombohedral axis (R3c space group), in which the Bi and Fe atoms have a quantitatively similar participation.

Thus, we found pressure favors two main modifications of the usual R3c phase, namely, a change in Bi's coordination and a low- or null-spin configuration of the  $\text{Fe}^{3+}$  ions. We also checked such variations can exist independently (e.g., LS  $\text{Fe}^{3+}$  can occur in absence of planar  $\text{BiO}_3$  groups), which gives rise to various metastable phases. Indeed, we obtained many metastable phases (not shown here) with different atomic and electronic structures, including the occurrence of intermediate-spin  $\text{Fe}^{3+}$ . We even found a mixed-spin phase, with one HS iron and one LS iron in our 10-atom cell, that becomes stable in the 35{37 GPa pressure range.

Metallization at the HS{LS transition. As expected, for the HS phase we obtained an AFM insulating ground state. The energy difference between the AFM and ferromagnetic (FM) configurations varies from about

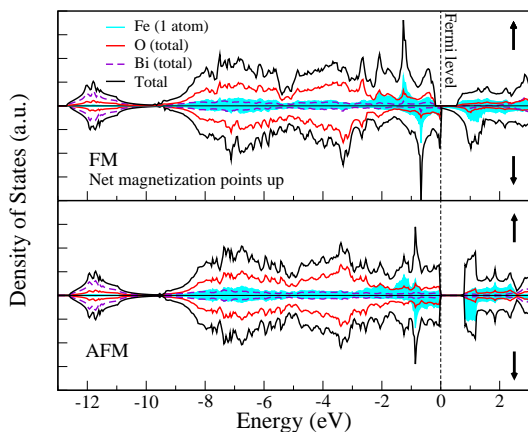


FIG. 4: (color online). Electronic density of states of the FM and AFM configurations of the LS phase of BFO at 50 GPa. The shaded area indicates the result for one  $\text{Fe}^{3+}$  ion with its local magnetic moment pointing up.

0.27 eV/f.u. at 0 GPa to about 0.65 eV/f.u. at 36 GPa, which is compatible with the experimentally observed high transition temperature ( $T_{\text{NeeL}} = 643$  K at 0 GPa) and its increase with pressure [1]. As shown in Fig. 2e, the HS phase is an insulator throughout its stability range, and its energy gap decreases with pressure.

According to our results, the properties of the LS phase are more complex. Throughout its stability range, the AFM and FM magnetic arrangements are nearly degenerate, never differing by more than 0.03 eV/f.u. (Moreover, the ground state shifts from AFM to FM as pressure increases.) This implies that the magnetic ordering temperature for the LS phase will be much (about 10 times) smaller than that of the HS phase. We also found the electronic structure of the LS phase depends strongly on the magnetic order. Figure 4 shows illustrative results at 50 GPa: The AFM case presents a gap of about 0.8 eV, while for the FM order we get a half-metallic solution.

These results imply that, if we were able to heat the LS phase up to room temperature ( $T_{\text{room}}$ ), we would obtain a paramagnetic state. Further, this magnetically-disordered phase will appear as being metallic, since the thermally-averaged equilibrium state will present a significant electronic density of states at the Fermi level. Thus, our calculations suggest that, at  $T_{\text{room}}$ , BFO might undergo a pressure-driven HS{LS transition that brings about simultaneous structural, magnetic, and electronic (insulator-to-metal) transformations.

Discussion. The picture of the HS{LS transition that emerges from our simulations is essentially identical to the one suggested by Gavriluk et al. [7] to explain their observed pressure-driven transition. One should keep in mind, though, that the experiments of Ref. 7 were performed at  $T_{\text{room}}$ ; thus, the identification between the experimental transition and our HS{LS transition relies on the assumption that our LS phase is the equilibrium state

at  $T_{\text{room}}$ .

To resolve this issue, one would need to compute the temperature-pressure ( $T$ - $P$ ) phase diagram of BFO *ab initio*, which falls beyond the scope of this work. Yet, we can estimate the temperature stability range of the low- $T$  phases by calculating their enthalpy difference with the cubic phase, as such a quantity should be roughly proportional to the temperature at which the transition to the cubic phase occurs. At 0 GPa we obtained 0.88 eV/f.u. for the difference between the R3c HS phase and the lowest-lying cubic phase (which presents  $\text{Fe}^{3+}$  in a HS state), a large value consistent with the experimentally observed high transition temperature (1200 K) [4, 16]. This enthalpy difference decreases gently with pressure: For example, at 50 GPa, the R3c LS phase and the lowest-lying cubic phase (which presents  $\text{Fe}^{3+}$  in a LS state) differ by about 0.60 eV/f.u. Hence, our calculations suggest that, within the stability range of the LS phase, the transition into a LS cubic phase will occur at temperatures well above  $T_{\text{room}}$  (roughly, in the 700–800 K range). Our results thus support the hypothesis of Gavriluk et al. that the metallic phase observed experimentally at high pressures and  $T_{\text{room}}$  contains LS  $\text{Fe}^{3+}$ .

We found additional support for this identification. The computed HS{LS transition pressure (about 36 GPa) agrees reasonably well with the observed one (40–50 GPa), and the wealth of competing (meta)stable phases that we found is consistent with the diffuseness of the experimental transition. Further, the results for  $V(P)$  in Fig. 2b are in good qualitative agreement with the experimental data, and the computed bulk modulus of the HS and LS phases are markedly different (the HS phase being significantly softer (as observed experimentally for the low- and high-pressure phases [17]). Finally, the pressure dependence of the enthalpy difference between the low- and high-pressure phases was experimentally determined to be 12 meV/GPa at the transition region, and we obtain about 15 meV/GPa.

It is not our purpose here to give a detailed electronic picture of the HS{LS transition that we found. Let us just note our results for BFO strongly resemble what occurs in hematite ( $\text{Fe}_2\text{O}_3$ ), which undergoes a HS{LS transition with accompanying metallization at 50 GPa [18, 19, 20]. Indeed, the conclusion of Ref. 20 that there is an enhancement of the metallic character of hematite's LS phase under pressure, driven by the broadening of the not-fully-occupied  $t_{2g}$  bands of  $\text{Fe}^{3+}$ , seems consistent with our findings. We should also note Gavriluk et al. have recently described the pressure-induced metallization in BFO in terms of a Mottn-Hubbard picture [8]. We have doubts about this interpretation: First-principles calculations show that BFO displays broad, significantly hybridized, valence bands (see Refs. 13 and 21 for the usual HS phase of BFO and Fig. 4 for our LS phase), which suggests it may not be adequate to place this material on the Mottn-Hubbard side of the usual

Zaanen-Sawatzky-A llen diagram [22].

Our results allow us to discuss currently debated features of the T-P phase diagram of BFO. Following the discovery of the high-temperature metallic phase mentioned above [4], which has the ideal cubic perovskite structure with a 5-atom unit cell, it has been proposed this phase might extend its stability range down to low temperatures and high pressures [1, 23]. Our results suggest to the contrary. While restricted to a 10-atom cell, our simulations do include the ideal cubic perovskite as a possible solution, and show this phase does not become the ground state under compression. For pressures extending up to 100 GPa, we always observe symmetry-lowering distortions, associated to oxygen-octahedron tiltings and the stereochemical activity of Bi. This prediction is consistent with the experimental results of Gavriliuk et al. [7] and Haumont et al. [24], who observe a non-cubic phase at high pressures and room temperature.

Finally, let us comment on the status of our quantitative results. As mentioned above, we repeated all our calculations for different values of the U parameter that defines the LDA+U functional. For the U values typically used in studies of BFO [13, 14, 25] and other oxides with  $\text{Fe}^{3+}$  [19] (i.e., in the 3{4 eV range), the obtained qualitative results are identical. At the quantitative level, the main difference is a positive shift of the transition pressures as U increases. For example, for U = 4 eV the HS{LS transition occurs at 42 GPa, as compared with 36 GPa for U = 3 eV. The differences are greater for the LS{NS transition, which occurs at about 130 GPa for U = 4 eV. This is not surprising, as a bigger value of U will tend to favor more insulating solutions. Hence, we think we can take our quantitative results as quite approximate in what regards the HS{LS transition and the properties of the HS and LS phases. The LS{NS transition pressure is, obviously, not well determined.

In summary, we have revealed and explained the occurrence of a manifold (structural/electronic/magnetic) phase transition in  $\text{BiFeO}_3$  at pressures of about 40 GPa. We hope our results will contribute to a better understanding of  $\text{BiFeO}_3$ 's T-P phase diagram and the complex interactions at work in this material.

We acknowledge fruitful discussions with G. Catalan, J. K. Reisel, and J.F. Scott. This work funded by M. A. C. M. U. F. i. (STREP\_FP 6-03321). It was also supported by C. S. I. C. (PIE-200760I015) and the Spanish (FIS2006-12117-C04-01, CSD2007-00041) and Catalan (SGR2005-683) Governments. We used the CESGA computing center.

[1] G. Catalan and J.F. Scott, *Adv. Mats.* (in press).

[2] See e.g. the strain-induced polarization rotation reported

- by Jang et al. [*Phys. Rev. Lett.* 101, 107602 (2008)].
- [3] P. Ravindran, R. Vidyasastry, A. Kjekshus, H. Fjellvåg, and O. Eriksson, *Phys. Rev. B* 74, 224412 (2006).
- [4] R. Palai et al., *Phys. Rev. B* 77, 014110 (2008).
- [5] R. Ramesh et al., *Nat. Mats.* (in press).
- [6] M. K. Singh, W. P. Reiller, M. P. Singh, R. S. Katiyar, and J.F. Scott, *Phys. Rev. B* 77, 144403 (2008).
- [7] A. G. Gavriliuk, V. V. Struzhkin, I. S. Lyubutin, M. Y. Hu, and H. K. Mao, *JETP Letts.* 82, 224 (2005); A. G. Gavriliuk, V. V. Struzhkin, I. S. Lyubutin, and I. A. Troyan, *JETP Letts.* 86, 197 (2007); A. G. Gavriliuk, I. S. Lyubutin, and V. V. Struzhkin, *JETP Letts.* 86, 532 (2007).
- [8] A. G. Gavriliuk et al., *Phys. Rev. B* 77, 155112 (2008).
- [9] J.P. Perdew and A. Zunger, *Phys. Rev. B* 23, 5048 (1981); D.M. Ceperley and B.J. Alder, *Phys. Rev. Lett.* 45, 566 (1980).
- [10] G. Kresse and J. Furthmüller, *Phys. Rev. B* 54, 11169 (1996); P.E. Blochl, *Phys. Rev. B* 50, 17953 (1994); G. Kresse and D. Joubert, *Phys. Rev. B* 59, 1758 (1999).
- [11] S.L. Dudarev, G.A. Botton, S.Y. Savrasov, C.J. Humphreys, and A.P. Sutton, *Phys. Rev. B* 57, 1505 (1998).
- [12] We used the PAW scheme [10], solving for the following electrons: Fe's 3d, and 4s, Bi's 6s, and 6p, and O's 2s and 2p; 400 eV plane-wave cut-off; centered 7 7 7 k-point grid for Brillouin Zone integrals. Calculation conditions checked to be converged. For BFO at 0 GPa we reproduce previous first-principles results [3, 13].
- [13] J.B. Neaton, C. Ederer, U.V. Waghmare, N.A. Spaldin, and K.M. Rabe, *Phys. Rev. B* 71, 014113 (2005).
- [14] C. Ederer and N.A. Spaldin, *Phys. Rev. B* 71, 060401(R) (2005).
- [15] M. Imada, A. Fujimori, and Y. Tokura, *Rev. Mod. Phys.* 70, 1039 (1998).
- [16] The 1200 K transition to the cubic phase does not proceed from the R3c phase stable at low temperatures, but from an intermediate phase [4]. Yet, those 1200 K measure the strength of the symmetry-lowering distortions in BFO, and it seems reasonable to correlate this quantity with our computed enthalpy difference.
- [17] The computed bulk modulus ( $B_0$ ) increases strongly with pressure. For the HS phase we have  $B_0 = 130\{300$  GPa within its stability range, and for the LS phase  $B_0 = 400\{500$  GPa. Gavriliuk et al. give a single value for their low- (76 GPa) and high-pressure (290 GPa) phases, which makes a comparison difficult. In fact, from the data in Ref. 7 we deduce  $B_0 = 180$  GPa for the low-pressure phase, a value much greater than the one (76 GPa) given by the authors themselves.
- [18] J. Badro et al., *Phys. Rev. Lett.* 89, 205504 (2002).
- [19] G. Rollmann, A. Rohrbach, P. Entel, and J. Hafner, *Phys. Rev. B* 69, 165107 (2004).
- [20] A.V. Kozhevnikov, A.V. Lukoyanov, V.I. Anisimov, and M.A. Korotin, *J. Exp. Theo. Phys.* 105, 1035 (2007).
- [21] S.J. Clark and J. Robertson, *Appl. Phys. Lett.* 90, 132903 (2007).
- [22] J. Zaanen, G.A. Sawatzky, and J.W. Allen, *Phys. Rev. Lett.* 55, 418 (1985).
- [23] J.F. Scott et al., *J. Am. Ceram. Soc.* 91, 1762 (2008).
- [24] R. Haumont et al., submitted.
- [25] I.A. Korneev, S. Lisenkov, R. Haumont, B. Dkhil, and L. Bellaiche, *Phys. Rev. Lett.* 99, 227602 (2007).